

## COMMUNICATION

# Modulating the crystal size and morphology of *in meso*-crystallized lysozyme by precisely controlling the water channel size of the hosting mesophase

Cite this: DOI: 10.1039/c2sm26988k

Received 27th August 2012  
Accepted 22nd October 2012

DOI: 10.1039/c2sm26988k

[www.rsc.org/softmatter](http://www.rsc.org/softmatter)

Alexandru Zabara and Raffaele Mezzenga\*

We explore the effects of increased protein mobility inside the aqueous channels of ordered lyotropic liquid crystals (LLC) of cubic *Pn3m* symmetry on the process of *in meso* crystallization of lysozyme proteins. The protein confinement within the channels is released by swelling the aqueous domains by doping the mesophase with a hydration-modulating agent that causes a near twofold increase in the diameter of the water channels. By means of small angle X-ray scattering and cross-polarized optical microscopy, we then show that increased diffusion of both protein and water molecules within the bulk hosting LLC leads to the formation of not only larger protein crystals but also crystals belonging to different polymorphic forms.

## Introduction

Lyotropic liquid crystals (LLC), based on the spontaneous self-assembly of neutral lipids in an aqueous medium, have been extensively studied in the past decades due to their ability to form ordered, complex fluidic systems based on liquid crystalline supramolecular architectures (such as lamellar, inverted hexagonal, and bicontinuous cubic).<sup>1–8</sup> These unique properties make them ideal candidates for a large number of practical applications in a variety of fields ranging from biomedical<sup>3</sup> and food technology<sup>4,7,8</sup> to pharmaceuticals,<sup>4</sup> drug delivery<sup>3,4</sup> and structural biology.<sup>5,6</sup> In particular, both the hydrophobic and the aqueous domains of the LLC have been extensively exploited for encapsulation and controlled release of various biomolecules, ranging from lipophilic and hydrophilic drugs,<sup>9,10</sup> to amino acids,<sup>11,12</sup> peptides,<sup>4,11</sup> and nucleic acids,<sup>11,13</sup> further emphasizing their potential use as delivery systems for target compounds.

Furthermore, due to their unique and remarkable resemblances to cellular membranes,<sup>14</sup> inverted LLC cubic phases provide structural biologists with a feasible, alternate tool in their crystallization methods, referred to as *in meso* crystallization.<sup>5,6,15</sup> Ever since its discovery, almost two decades ago,<sup>15</sup> this novel approach to membrane protein crystallization has been steadily gaining ground

in the field of structural biology, being responsible for a large number of high-resolution structures<sup>5,6,16,17</sup> and culminating with the resolution of the transmembrane proteins G Protein Coupled Receptors (GPCR).<sup>18</sup>

The dual polar/apolar nature of the hosting mesophase allows for the crystallization of both globular and membrane proteins, since hydrophilic proteins can be encapsulated relatively easily within the water channels of the hosting mesophase, from which they can readily nucleate and further allow crystal growth. This was clearly shown by several recent reports concerning solubilization of globular proteins inside the aqueous domains of the LLC<sup>19–23</sup> (such as  $\alpha$ -chymotrypsin, lysozyme, and cytochrome c) as well as crystallization of small hydrophilic proteins in both the inverted hexagonal and bicontinuous cubic phases.<sup>24,25</sup>

In a previous study,<sup>26</sup> we have systematically explored the complex mechanisms of the *in meso* crystallization process using monoglycerides and lysozyme as a model system. We have investigated how the initial structure and symmetry of the hosting mesophase, as well as the available amount of water in the system (bulk vs. excess water conditions), can affect the polymorphic state of *in meso* crystallized lysozyme. In particular, we showed the possibility of engineering protein crystals at a molecular and macroscopic level by varying the initial symmetry of the hosting mesophase, as a means of tuning the size of the water domains.

In this work, we use a different strategy to precisely control the diameter of the nanofluidic aqueous channels, while maintaining fixed the space group of the hosting mesophase to a reverse *Pn3m* cubic phase. To do so we blend the monoglyceride lipid host, monolinolein (MLO), with a hydration enhancing agent (*e.g.* octyl glucoside). In a recent work, we have already demonstrated that this route allows increasing water channels and gives access to the crystallization of an unprecedented class of large hydrophilic proteins ( $\beta$ -lactoglobulin, thaumatin and porcine pancreatic elastase, with a diameter of 52 Å, 59 Å and 64 Å, respectively).<sup>30</sup> Here we clearly show that the same route enables the formation of larger protein crystals with a rich and tunable crystal polymorphism, and this, without the need of changing the symmetry of the host

ETH Zurich, Food & Soft Materials Science, Schmelzbergstrasse 9, LFO, E23, 8092 Zürich, Switzerland. E-mail: [raffaele.mezzenga@hest.ethz.ch](mailto:raffaele.mezzenga@hest.ethz.ch)

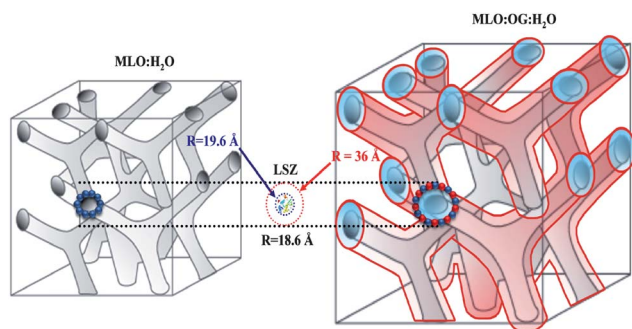


**Fig. 1** Schematic concept of the *in meso* crystallization of lysozyme from within the aqueous domains of the two studied hosting systems. The larger size of the MLO:OG:H<sub>2</sub>O system allows for a better diffusion of protein molecules and thus modulating the final polymorphic state of the *in meso* grown lysozyme crystals.

mesophase, can further widen the applicability of *in meso* crystallization methods in the design of protein crystals.

## Results and discussion

The relatively small size of the LLC aqueous channels has always been the limiting factor,<sup>17</sup> restricting the mesophases' ability to function as hosting reservoirs for protein crystallization. However, we have recently shown that doping the lipidic system with a hydration modulating agent such as octyl glucoside (OG)<sup>27–29</sup> leads to a sufficiently large increase in the diameter of its water channels (from 39 Å to 72 Å) to allow the possibility of assisting *in meso* crystallization of a wide class of previously inaccessible proteins.<sup>30</sup> It therefore seemed reasonable to assume that increasing the size of the aqueous channels and consequently the diffusion rates of both water and protein molecules while maintaining identical symmetry of the hosting mesophases would have an impact on protein crystal growth and morphology (Fig. 1).

The evidence for the increase in aqueous domain size and the physical origin of this increase are presented in Fig. 2a–c. Fig. 2a

shows the small angle X-ray scattering (SAXS) spectra of scattered intensities *versus* scattering vector  $q$ , azimuthally averaged into 1D profiles for the two cases studied, monolinolein:water (blue spectra) and the same system doped with the hydration enhancing agent, octyl glucoside, in a 9 : 1 molar : molar (monolinolein : OG) ratio (red spectra) under the conditions of maximum hydration (37% water for the MLO:H<sub>2</sub>O system and 57% water for the case of MLO:OG:H<sub>2</sub>O). In these conditions, just prior to coexistence with excess water, the radii of the water channels in the chosen systems should have reached their maximum possible values. In both cases SAXS diffraction peaks (in the ratios of  $\sqrt{2}$ ,  $\sqrt{3}$ ,  $\sqrt{4}$ ,  $\sqrt{6}$ ,  $\sqrt{8}$ ,  $\sqrt{9}$ ) and cross-polarized visual observation (which revealed no signs of turbidity) indicated a  $Pn3m$  double diamond bulk cubic phase. Analysis of the structural parameters (Fig. 2b) showed a 35% increase in the size of the lattice parameter (from 95 to 128 Å) and an almost two-fold increase in water channel size (from 39 to 72 Å, calculated as in (ref. 8)) for the MLO:OG:H<sub>2</sub>O doped mesophase, which would therefore allow a much faster rate of diffusion for both protein and water molecules in the system. Fig. 2c illustrates the physical origin of this large increase in structural parameters, by comparing the phase diagrams of the two studied systems (MLO:H<sub>2</sub>O and MLO:OG:H<sub>2</sub>O). In both cases the order-to-order transitions followed a similar sequence,  $L_{\alpha} \rightarrow L_{\alpha} + Ia3d \rightarrow Ia3d \rightarrow Pn3m \rightarrow Pn3m + H_2O$ , in perfect agreement with previous findings for the monoglyceride:water system,<sup>8</sup> with the clear distinction, however, that in the case of the MLO:OG system, all transitions were systematically shifted towards higher hydration. Thus, by the time the boundary with excess water is reached in the doped system, the associated  $Pn3m$  cubic phase contains a much larger quantity of water, which in turn is responsible for the inherent increase in water channel size.

Assessment of protein loading effects in time (5 wt% lysozyme was loaded into the mesophase prior to crystallization) on the structure and symmetry of the doped hosting system (MLO:OG:H<sub>2</sub>O) was made by means of small angle X-ray scattering,

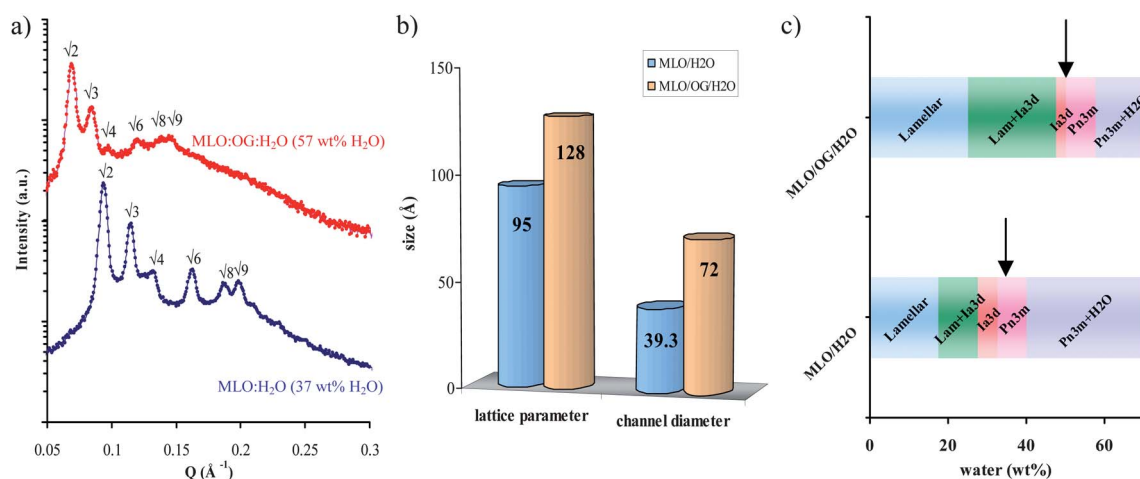


**Fig. 2** Evidence for the increase in the structural parameters of the doped mesophase (MLO:OG:H<sub>2</sub>O) and the physical origin of the swelling: (a) 1D small angle X-ray scattering spectra of scattered intensities *versus* scattering vector  $q$  for the two systems used (MLO:H<sub>2</sub>O – blue; MLO:OG:H<sub>2</sub>O – red); (b) analysis of the structural parameters for the two systems; (c) phase diagrams obtained for the two systems at a fixed temperature of 20 °C (the initial positions, within the phase diagrams, of the protein-loaded mesophases prior to crystallization are depicted by black arrows).

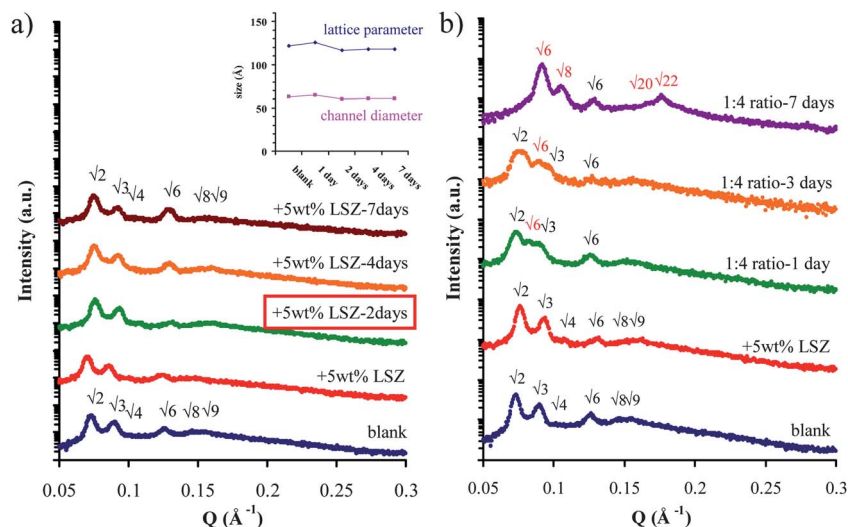


**Fig. 3** 1D SAXS spectra showing (a) the effects in time of protein loading on the structural parameters of the MLO:OG:H<sub>2</sub>O hosting mesophase (the time at the onset of crystallization is highlighted in red); (b) time-evolution of the structure and symmetry of the hosting phase during the crystallization process at a ratio of 4 : 1 mesophase : crystallization buffer.

as shown in Fig. 3a. Although the hosting mesophase maintained its initial  $Pn3m$  cubic symmetry in time (as shown by the diffraction peak ratio), protein loading produced a slight swelling ( $\sim 2$  Å in diameter) of the water channels during the first day of incubation followed, upon equilibration of the system (after two days – moment in time chosen for the beginning of protein crystallization), by a moderate decrease of the structural parameters ( $\sim 9$  Å in the lattice parameter and 4 Å in the water channel diameter), associated with the dehydration of the lipidic system by the protein molecules. This has similarities with the findings reported in our previous report, where the lysozyme was confined in the tighter channels of the nondoped MLO:H<sub>2</sub>O system.<sup>26</sup>

The crystallization kinetics for a ratio of mesophase to crystallization buffer of 4 : 1 (ratio capable of maintaining a bulk phase throughout the crystallization process) is followed in Fig. 3b. The 1D SAXS spectra reveal a transition of the system, over several days, from the initial double diamond cubic symmetry to coexistence of double diamond  $Pn3m$  and gyroid  $Ia3d$  cubic phases, as shown from the appearance of the  $\sqrt{6}$   $Ia3d$  peak at early stages and higher order Bragg reflections of the  $Ia3d$  appearing with increasing equilibration time. This is the signature of the de-hydration process of the mesophase caused by the nucleation and growth of lysozyme crystals and is in good correlation with our previous findings on the undoped MLO:H<sub>2</sub>O mesophase system.<sup>26</sup>

Cross-polarized optical microscopy was used to monitor crystal growth and to assess the morphology of the lysozyme crystals obtained under the different conditions explored (bulk phase vs. excess water – Fig. 4). Furthermore it allowed us to assess and compare the different crystal polymorphs obtained using either the doped mesophase (MLO:OG:H<sub>2</sub>O) or the classic MLO:H<sub>2</sub>O system, evaluating the influence of the increased water channel size on both size and protein crystal morphology.

From our earlier observations of *in meso* crystallization we know that the initial structure and symmetry of the hosting phase and its position within the phase diagram play a major role in the process

of crystal growth and modulation of the final protein crystal polymorphisms.<sup>26</sup> It can then be inferred that an increase in water channel size directly correlates with the space group of the protein crystals, although the simultaneous change in the symmetry of the host mesophase does not allow us to disentangle the effects of mesophase symmetry and water channel size. The possibility of changing the water channel size without altering the mesophase symmetry of the MLO:OG:H<sub>2</sub>O now enables this point to be univocally assessed.

A first inspection of microscopy images of the *in meso*-crystallized lysozyme (Fig. 4) revealed that the increase in the water channel diameter led to the formation of considerably larger protein crystals as compared to those grown in the MLO:H<sub>2</sub>O cubic phase, regardless of the total amount of water available in the system, *e.g.* in both bulk phase and excess water conditions.

More importantly, releasing the confinement of the lysozyme molecules within the mesophase water channels, when swelling them in the presence of the OG surfactants, had a direct impact on the final symmetry of the *in meso*-grown protein crystals.

When excess water was available in the system, no effect was found on the symmetry of the lysozyme crystals, which were always of the tetragonal space group, independently of the presence or not of the OG co-surfactants. This indicates that under these conditions, the lysozyme crystals always bear the same symmetry as that of proteins crystallized in free, unconstrained buffer conditions.

On the other hand, in the bulk  $Pn3m$  phase, two different polymorphisms of *in meso* lysozyme crystals were found. In the confined conditions offered by the MLO:H<sub>2</sub>O mesophase, where the water channel diameter just exceeds the hydrodynamic diameter of the protein, lysozyme was found to crystallize into an orthorhombic crystal symmetry (space group  $P2_12_12_1$ ). The doped system (MLO:OG:H<sub>2</sub>O), on the other hand, produced again and exclusively large lysozyme crystals of the tetragonal symmetry (space group  $P4_32_12$ ), as a result of the increased degrees of freedom of lysozymes within the swollen water channels. Thus, it can be unambiguously

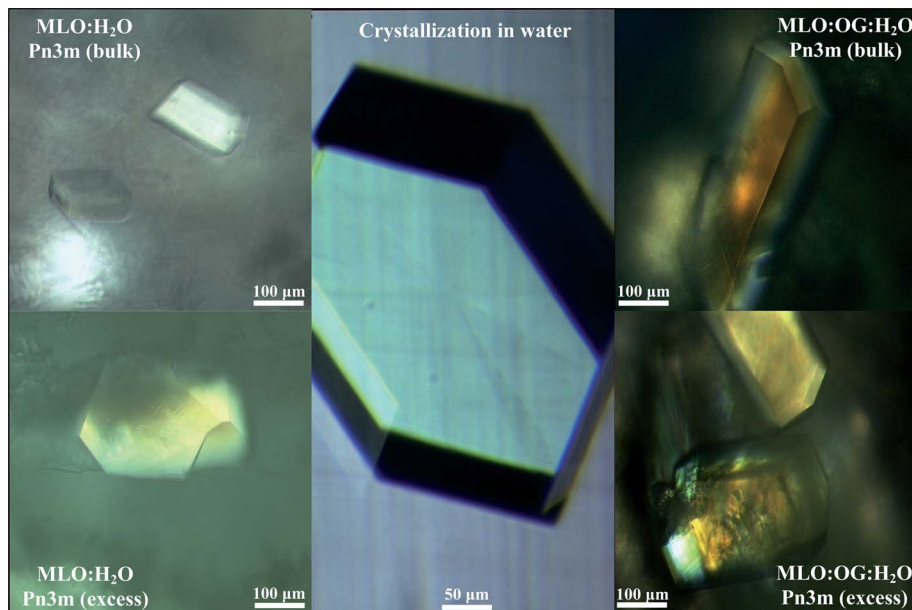


**Fig. 4** Cross-polarized optical microscopy images of the lysozyme crystals obtained *in meso*. For the MLO:H<sub>2</sub>O system (left side) the protein crystals show orthorhombic symmetry (space group  $P2_12_12_1$ ) for bulk phase crystallization and tetragonal symmetry (space group  $P4_32_12$ ) for crystallization under excess water conditions. For the doped mesophase MLO:OG:H<sub>2</sub>O (right side), the lysozyme crystals obtained show a tetragonal symmetry (space group  $P4_32_12$ ) in both bulk and excess water conditions.

concluded that increasing the size of the aqueous channels allows “free” crystallization to occur within the hosting mesophase, creating the favorable environment needed for protein molecules to nucleate and form larger and higher quality crystals.

## Materials and methods

### Materials

Dimodan U/J was a gift from Danisco (Denmark) and was used as received. This commercial-grade form of monolinolein (MLO) contains more than 98 wt% monoglyceride. The same batch of Dimodan was used throughout the whole work. Octyl glucoside (OG) was purchased from Sigma-Aldrich (Buchs, Switzerland). Chicken egg-white lysozyme (LSZ) was purchased from Sigma-Aldrich (Schnelldorf, Germany). All the necessary salts for the crystallization procedures were purchased from Sigma Aldrich-Chemie (Steinheim, Germany). Linbro 24-well hanging drop crystallization plates as well as all other crystallization accessories were purchased from Jena Bioscience (Jena, Germany).

### Sample preparation

The composition of each LLC system (empty and loaded) with or without the added doping agent was as follows: in the case of LLC loaded with protein, 5 wt% LSZ was dispersed in water prior to its incorporation into the LC mesophases. The cubic phase ( $Pn3m$ ) contained 65.3 wt% MLO and 34.7 wt% protein buffer (or LSZ solution) for the MLO:H<sub>2</sub>O system and 51 wt% MLO : OG (mixed in a 9 : 1 molar : molar ratio) and 49 wt% protein buffer (or LSZ solution) for the system doped with octyl glucoside. The liquid crystalline mesophases were prepared by mixing weighed quantities of monoglyceride and protein solution (protein buffer in the case of empty phases), followed by heating to 45 °C and vortexing until a

homogeneous mixture was obtained. The prepared mesophase was then allowed to cool down to room temperature.

All the buffers and protein solutions were prepared using ultra-pure water and the pH was adjusted using a 1 M solution of HCl.

### Crystallization of chicken egg-white lysozyme

LSZ crystals were grown at 20 °C using the hanging drop vapor diffusion method. The reservoir solution contained 500 μL of 0.1 M Na acetate buffer (pH 4.5) and 0.8 M NaCl. The drop for the control experiments contained 4 μL of 50 mg mL<sup>-1</sup> LSZ solution in sodium acetate buffer and 1 or 2 μL of the reservoir solution (for the different mixing ratios). The drops for *in meso* crystallization were prepared as follows. Protein solutions were mixed with melted Dimodan in sealed Pyrex glass tubes. This pre-crystallization mix consisted of approximately 51% (w/w) MLO:OG and 49% (w/w) protein solution. The pre-crystallization mix was then dispensed on 22 mm siliconized glass cover slides in layers of 1 to 1.5 mm thickness, and the amount dispensed was weighted. A proportionally small amount of the respective crystallization buffer (according to the desired ratio 1 : 4) was then added on top of the protein-loaded mesophase layer to provide the necessary initial crystallization salt. A much larger reservoir (containing 500 μL of crystallization buffer), not in contact with the mesophase, was used to allow water vapour osmotic re-equilibration between the mesophase and the reservoir crystallization buffer. The glass slides containing the final mix were then inverted above their respective wells and sealed.

### Cross-polarized optical microscopy

Microscopy observations regarding protein crystal growth and morphology were achieved under cross-polarized light using a Zeiss

Axioskop 2 MOT optical microscope and a magnification of 10 $\times$ . All the pictures were taken with a Hamamatsu C5810 CCD camera.

### Small angle and wide angle X-ray scattering

Small angle X-ray scattering experiments were performed on a MicroMax-002+ microfocussed beam, operating at a voltage and filament current of 45 kV and 0.88 mA, respectively. The Ni-filtered Cu K $\alpha$  radiation ( $\lambda_{\text{Cu K}\alpha} = 1.5418 \text{ \AA}$ ) was collimated by three pinhole (0.4, 0.3 and 0.8 mm) collimators and the data were collected by a two dimensional argon-filled Triton detector. An effective scattering-vector range of  $0.03 \text{ \AA}^{-1} < q < 0.45 \text{ \AA}^{-1}$  was probed, where  $q$  is the scattering wave-vector defined as  $q = 4\pi\sin(\theta)/\lambda_{\text{Cu K}\alpha}$  with a scattering angle of  $2\theta$ . For all measurements the samples were placed inside a Linkam HFS91 stage specially designed for X-ray scattering measurements.

### Conclusions

In summary, the present work brings further insights into the process of *in meso* crystallization by showing the close interplay between the size of the ordered aqueous domains of the LLC and the intricate process of crystal growth. To this point we clearly demonstrate that a less constricted diffusion of protein molecules within the bulk hosting phase leads to the formation of larger *in meso* protein crystals comparable to those obtained by crystallization in water (e.g. without the presence of the confining lipidic mesophase).

### References

- 1 R. Mezzenga, P. Schurtenberger, A. Burbidge and M. Michel, *Nat. Mater.*, 2005, **4**, 729–740.
- 2 A. Yagmur and O. Glatter, *Adv. Colloid Interface Sci.*, 2009, **147–148**, 333–342.
- 3 A. Fehér, E. Urbán, I. Erős, P. Szabó-Révész and E. Csányi, *Int. J. Pharm.*, 2008, **358**, 23–26.
- 4 M. Cohen-Avrahami, A. Aserin and N. Garti, *Colloids Surf., B*, 2010, **77**, 131–138.
- 5 M. Caffrey and V. Cherezov, *Nat. Protoc.*, 2009, **4**, 706–731.
- 6 M. Caffrey, *J. Struct. Biol.*, 2003, **142**, 108–132.
- 7 K. Larsson, *Curr. Opin. Colloid Interface Sci.*, 2000, **5**, 64–69.
- 8 R. Mezzenga, M. Grigorov, Z. Zhang, C. Servais, L. Sagalowicz, A. I. Romoscanu, V. Khanna and C. Meyer, *Langmuir*, 2005, **21**, 6165–6169.
- 9 J. C. Shah, Y. Sadhale and D. M. Chilukuri, *Adv. Drug Delivery Rev.*, 2001, **47**, 229–250.
- 10 R. Negrini and R. Mezzenga, *Langmuir*, 2011, **27**, 5296–5303.
- 11 J. Clogston and M. Caffrey, *J. Controlled Release*, 2005, **107**, 97–111.
- 12 S. Z. Mohammady, M. Pouzot and R. Mezzenga, *Biophys. J.*, 2009, **96**, 1537–1546.
- 13 I. Amar-Yuli, J. Adamcik, S. Blau, A. Aserin, N. Garti and R. Mezzenga, *Soft Matter*, 2011, **7**, 8162–8168.
- 14 Z. A. Almsheerqi, S. D. Kohlwein and Y. Deng, *J. Cell Biol.*, 2006, **173**, 839–844.
- 15 E. M. Landau and J. P. Rosenbusch, *Proc. Natl. Acad. Sci. U. S. A.*, 1996, **93**, 14532–14535.
- 16 V. Cherezov, E. Yamashita, W. Liu, M. Zhalnina, W. A. Cramer and M. Caffrey, *J. Mol. Biol.*, 2006, **364**, 716–734.
- 17 M. Caffrey, *Biochem. Soc. Trans.*, 2011, **39**, 725–732.
- 18 D. M. Rosenbaum, C. Zhang, J. A. Lyons, R. Holl, D. Aragao, D. H. Arlow, S. G. F. Rasmussen, H.-J. Choi, B. T. DeVree, R. K. Sunahara, P. S. Chae, S. H. Gellman, R. O. Dror, D. E. Shaw, W. I. Weis, M. Caffrey, P. Gmeiner and B. K.obilka, *Nature*, 2011, **469**, 236–240.
- 19 J. Kraineva, C. Nicolini, P. Thiyagarajan, E. Kondrashkina and R. Winter, *Biochim. Biophys. Acta*, 2006, **1764**, 424–433.
- 20 V. Razumas, K. Larsson, Y. Mieziš and T. Nylander, *J. Phys. Chem.*, 1996, **100**, 11766–11774.
- 21 C. E. Conn, C. Darmanin, S. M. Sagnella, X. Mulet, T. L. Greaves, J. N. Varghese and C. J. mesomond, *Soft Matter*, 2010, **6**, 4828–4837.
- 22 C. E. Conn, C. Darmanin, S. M. Sagnella, X. Mulet, T. L. Greaves, J. N. Varghese and C. J. Drummond, *Soft Matter*, 2010, **6**, 4838–4846.
- 23 R. M. Epand, *Biochim. Biophys. Acta*, 1998, **1376**, 353–368.
- 24 E. M. Landau, G. Rummel, S. W. Cowan-Jacob and J. P. Rosenbusch, *J. Phys. Chem. B*, 1997, **101**, 1935–1937.
- 25 T. Mishraki, D. Libster, A. Aserin and N. Garti, *Colloids Surf., B*, 2010, **75**, 391–397.
- 26 A. Zabara, I. Amar-Yuli and R. Mezzenga, *Langmuir*, 2011, **27**, 6418–6425.
- 27 B. Angelov, A. Angelova, M. Ollivon, C. Bourgaux and A. Campitelli, *J. Am. Chem. Soc.*, 2003, **125**, 7188–7189.
- 28 B. Angelov, A. Angelova, V. M. Garamus, G. Lebas, S. Lesieur, M. Ollivon, S. S. Funari, R. Willumeit and P. Couvreur, *J. Am. Chem. Soc.*, 2007, **129**, 13474–13479.
- 29 A. Angelova, B. Angelov, R. Mutafchieva, S. Lesieur and P. Couvreur, *Acc. Chem. Res.*, 2011, **44**, 147–156.
- 30 A. Zabara and R. Mezzenga, *Soft Matter*, 2012, **8**, 6535–6541.